ORIGINAL RESEARCH

Influence of hydroxyethyl and carboxymethyl celluloses on the rheology, water retention and surface tension of water-suspended microfibrillated cellulose

Vanja Kokol

Abstract Water-soluble polymers have been shown to improve the flow rigidity and water retention ability of highly-branched (flocculated) and polydisperse water-suspended MFC, thereby also modifying and controlling their rheological behaviour. The addition of hydroxyethyl (HEC) and carboxymethyl (CMC) celluloses of different content (5–10–20 w/w%), molecular weights (M_W, 90.000–1.300.000 g/mol) and degrees of substitutions (DS, 0.7–1.2) to 1.5 wt% MFC suspension, have thus been studied by evaluating their microstructure (SEM imaging), strength and rheological properties, i.e. the yield stress and flow under rotational (viscosity vs. shear rate) and oscillatory (viscoelastic) regime, using cone-plate measuring geometry at a rather low truncation gap. The pure MFC suspension showed high-viscosity at lower shear stress and shear-thinning behaviour at higher rates, with two yielding zones, indicating a secondary deflocculation of smaller and more stiffly packed fibril structures and their orientation/aligning in the direction of flow. This behaviour was reduced substantially by the addition of high-M_W HEC, or almost eliminated completely by medium-M_W CMCs with higher DS, yielding suspensions with higher and stability-prolonged zero-shear viscosity, as well as a more linearly decreased and irreversible viscosity profile after the shear load removal at higher shear stresses. The carboxylic groups at CMC additionally decreased the interactions between the fibrils, and subsequently reduced the fibrils' flocks, or formed larger aggregates with their integrations, while increasing the MFC suspension gel-strength, improving its flow and viscoelastic behaviour through higher water retention ability and surface tension properties, and also its recovery after deformation.

Keywords Microfibrillated cellulose · Hydroxyethyl and carboxymethyl cellulose · Viscosity · Viscoelasticity · Water retention · Surface tension

V. Kokol (✉)
Faculty of Mechanical Engineering, University of Maribor, Smetanova ul. 17, 2000 Maribor, Slovenia
e-mail: vanja.kokol@um.si

Introduction

The unique flow and viscoelastic characteristics of micro- and nano-fibrillated cellulose (MNFC) aqueous suspensions are becoming of high importance for both their handling and use during many emerging applications, such as thickening (Li et al. 2021; Dimic-Misic et al. 2013a), compounding (Clemons and Sabo 2021), fibre spinning (Lundahl et al. 2017), surface coating (Kumar et al. 2016a, 2017; Oh et al. 2017), as well as screen (Kokol et al. 2021) and digital (3D) printing (Wang et al. 2020; Mariani et al.

2019). During these processes the suspensions are exposed to complex loads, including a broad range of shear rates and stresses. Knowing how MNFC suspensions behave at both low (up to 10^3 s^{-1}) and high (between 10^3 and 10^6 s^{-1}) shear rates is, thus, an important characteristic, as its viscosity and flow behaviour determine their processing and structural recovery after elongational deformation (Iotti et al. 2011; Kumar et al. 2016b; Vadodaria et al. 2018; Jaiswal et al. 2021).

Besides MNFCs` solid content, substantial progress in understanding the rheological behaviour of MNFC suspensions by focusing on the fibrils` morphology (i.e. the fibrils` aspect ratio and network structure) and interactive forces (electrostatic/ionic repulsions and attractions, as well as physical interactions) between them, depending on the source of the cellulose raw material and manufacturing conditions (e.g. the degree of delamination during preparation), have, thus, been considered in many research articles in the last decade (Cinar Ciftci et al. 2020, Schenker et al. 2019; Siqueira et al. 2010; Nechyporchuk et al. 2016; Taheri and Samyn 2016). It has been established that as prepared MNFC water suspensions form highly viscous gels already at rather low (0.1–0.5 wt%) consistency (Cinar Ciftci et al. 2020; Facchine et al. 2020; Li et al. 2021) due to the fibrils` high specific surface area, and, thus, high hydroxyl group surface density with water trapping and hydrogen bonding properties. However, at steady shear conditions, the shear-thinning behaviour of nanofibrillated cellulose (NFC) suspensions at low solid content can be rather poor, as nanofibrils are mostly completely detached from each other, so there are no, or rare, branched or network structures present, except possible entanglements or agglomeration that is brought about by the attractive forces of differently surface-charged fibrils (Nechyporchuk et al. 2016; Naderi and Lindström 2014, 2015).

On the other hand, the rheological properties of highly branched or network-like micro-fibrillated cellulose (MFC) structures with a broader and rather heterogeneous fibrils` size distribution ranging from micro- to nanometers in diameter and micrometres in length (Nechyporchuk et al. 2014; Haavisto et al. 2015; Schenker et al. 2018; Shafiei-Sabet et al. 2016; Dimic-Misic et al. 2018; Cinar Ciftci et al. 2020), which gives rise to the formation of differently large and strong aggregates and agglomerates or floccules,

with colloidal and non-colloidal characteristics (Pääkkö et al. 2007) among the freely suspended, typically thinner and shorter, fibrils, respectively (Karppinen et al. 2012; Hubbe et al. 2017; Koponen 2000) which is much more complex. Due to the differently strong interfibrillar forces and fibrils` organisation (collision, entanglements and flocculation of fibrils during preparation/stirring; Saarikoski et al. 2012), MFC can, thus, form differently strong gel-like structures (Pääkkö et al. 2007), whose rheological behaviour, however, is dependent on the mechanism of connectivity and rigidity of these fibril clusters, as well as their separation and deformation during the increasing shear rates. Generally, MFC suspensions exhibit high viscosities at low shear rates, and a significant shear-thinning behaviour with increasing shear rates, while the viscosity increases, preferably with the fibrils` surface charging rather than with the increasing concentration of MFC (Vesterinen et al. 2010; Iotti et al. 2011; Karppinen et al. 2011; Moberg et al. 2017). A transition region (Karppinen et al. 2011) and a shear-rate viscosity hysteresis loop effect with a dilatant (non-Newtonian) behaviour at lower shear rates (usually up to 50 s^{-1}), has also been reported for most MFC suspensions, already from 1 wt% of solid content (Iotti et al. 2011; Yuan et al 2021), thus explaining the shear-induced structural changes of the initial aggregated / flocculated network structure by increasing the shearing. Additional studies (Saarikoski et al. 2012; Koponen 2000) also revealed that such a fibrils` flocculation network separates first into chain-like floc formations, and, by further shear rate increase, into individual spherical flocs, the size of which is inversely proportional to the shear rate, and dependent on the geometry gap affecting the measured shear stress. Indeed, by optical coherence tomography it was comfirmed that the rupture dynamics of flocs during shear-thinning is linked quantitatively to the decrease of the floc size for three consistency levels (Lauri et al. 2021). All such heterogeneous network structures of MFC suspensions also exhibit elastic characteristics (i.e., the storage modulus G' exceeds the loss modulus G''), where the storage modulus (determined from the stress or strain amplitude sweep) is not affected by the lower frequency, while resulting in its decrease by exceeding the critical stress (or strain) amplitude, being associated with the breakdown of its initial network structure (Karppinen et al. 2011).

The cellulose fibrils` surface characteristics, above all surface charge, causing electrostatic or ionic repulsion or attractions (Moberg et al. 2017; Naderi and Lindström 2014), and the presence of ions (Saarikoski et al. 2012; Naderi and Lindström 2015) have also received much attention, and have been encompassed in some recent rheological studies. While electrostatic repulsion, associated with the fibrils` surface charge, retards aggregation/mechanical entanglement and flocculated network formation, and, thus, lowering the viscosity and rheological response of MNCF water suspensions (Moberg et al. 2017; Naderi and Lindström 2014), an increased tendency to aggregation/flocculation in the presence of ions was revealed by decreasing the interfibrillar repulsion and encouraging aggregation, the disintegration of which in steady shear resulted in large free voids without fibrils appearing in the structure parallel to the direction of compression (Saarikoski et al. 2012). Furthermore, the addition of water-soluble polymers to the MFC suspension revealed that its microstructure (flocculation behaviour) and rheological properties could be modified and controlled. The addition of sodium carboxymethylcellulose thus made the MFC suspension less gel-like, and reduced the shear thinning, due to the more homogeneously spread and aligned microfibrils (Veen et al. 2015), whereas cationic polyacrylamide and starch strengthened the MFC gel and preserved its shear-thinning behaviour (Karppinen et al. 2011; Vesterinen et al. 2010).

In this study, the changing of 1.5 wt% water-suspended MFC microstructure after the addition of different amounts (5–10–20 wt% per wt% of MFC) of hydroxyethylated (HEC) and carboxylmethylated (CMC) cellulose polymers with different molecular weights (M_W, 90.000–1.300.000 g/mol) and degrees of substitutions of CMC (DS, 0.7–1.2), have been evaluated by microscopic imaging and rheological behaviour. In this frame, several rheological parameters, such as zero shear viscosity (η_0), yield point (τ_y), power parameters (K and N), flow point ($G' = G''$) and tan δ (tan $\delta = G''/G'$) of differently formulated MFC-based suspensions, were investigated by performing steady shear rotational (viscosity vs. shear rate) and oscillatory (viscoelastic) flow in amplitude and frequency sweep tests, respectively. The water retention and surface tension properties of the suspensions were evaluated in addition,.

Experimental

Materials

Commercially available microfibrillated cellulose, (MFC) Exilva F-01-L, consisting of approximately 22–50 μm long and up to 50 nm tight fibrils with negative surface charge of -28 ± 2.2 mV and 18.5 ± 4.0 mmol/kg, as determined by using conductometric titration, was provided by Borregaard AS, Norway. Analytical grade (Sigma Aldrich, Germany) carboxylmethyl cellulose (CMC) and hydroxyethyl cellulose (HEC) of different molecular weights (M_W) and degrees of substitution (DS) were used as presented in Table 1.

Preparation of MFC suspensions

The MFC-based suspensions were prepared by mixing the desired amount of water pre-dispersed MFC

Table 1 Characteristics of carboxylmethyl cellulose (CMC) and hydroxyethyl cellulose (HEC) used as water retention additives (according to the technical data sheet from Sigma-Aldrich)

Name (catalogue no.)	Average molecular weight, M_W (g/mol)	Degree of substitution, DS	Viscosity (mPas) at a given concent. (wt%), measured at 25 °C by a Brookfield LV spindle viscometer
HEC1 (434965)	90.000	–	750–1.500 (5 wt%)
HEC2 (434973)	720.000	–	45.000–65.000 (2 wt%)
HEC3 (434981)	1.300.000	–	34.000–50.000 (1 wt %)
CMC1 (419273)	90.000	0.7	50–200 (4 wt%)
CMC2 (419303)	250.000	0.8–0.9	400–800 (2 wt%)
CMC3 (419281)	250.000	1.2	2.500–6.000 (1 wt%)
CMC4 (419338)	700.000	0.8–0.95	2.500–6.000 (1 wt%)

and the desired amount of water pre-dissolved HEC or CMC. An amount of 8.8 wt% MFC was first diluted to about 1/3 by gradual addition of the required volume of distilled water, and mixing it in a 250 ml low-shaped glass cup by a three-bladed (5 cm in diameter) propeller mixer (RE 166 Analog IKA, Germany) from low speed (300 rpm) via medium (1000 rpm) to higher (2000 rpm) speeds, each for 15 min, and, after the addition of another 1/3 volume of water and repeating the mixing speeds, thus to obtain a homogeneous MFC suspension of known solid content. The required amount of HEC/CMC was pre-dissolved in distilled water by mixing it at 800 rpm using a magnetic stirrer at room temperature until the HEC/MFC was completely dissolved. Finally, an appropriate amount of pre-dispersed MFC was added by mixing them at 2500 rpm for 15 min, and another 30 min at 1500 rpm. In the final suspensions the concentration of MFC was 1.5 wt%, and CMC or HEC were added as 5–10–20 w/w% from the dry weight of MFC, or as 0.075–0.15–0.3 wt%. Before further analysis, the samples were left to rest for at least 10 min.

Scanning electron microscopy (SEM) imaging

The high resolution images of the selected MFC-based suspensions were performed using a Sirion 400NC (FEI, USA) microscope. A drop of each suspension (as prepared) was applied to the sample holder and air dried before the analysis. For each MFC suspension, up to ten SEM micrographs were performed at different magnifications, thus, to determine the water-suspended fibrils` microstructure credibly, as well as the fibrils' distribution and/or their aggregation.

Rheological evaluation

Rheological measurements of the prepared suspensions were performed at a constant temperature of 23 ± 1 °C by using a rotational rheometer Physica MCR 302 (Anton Paar GmbH, Austria) and a cone–plate measuring configuration with a cone of 50 mm in diameter and 1° angle (CP50/1°), and at a truncation gap of 0.1 mm; both the cone and plate had smooth surfaces. This (cone-plate) measuring system has generally proved to be less appropriate for investigation of the flow and viscoelastic properties of microfibrillated suspensions, because of being able to

cause rheometric-induced artefacts (side-effects) like wall depletion (ejection of larger fibrils` structures from the measurement gap/cell wall due to increased floc-floc interactions; Nazari et al. 2016), shear strips or water depletion and associated apparent slippage at the geometry walls, even at low (below 3 wt%) MFC concentrations, and, thus, might lead to misinterpretations of the rheograms (Schenker et al. 2018; Kumar et al. 2016b; Nazari et al. 2016; Naderi and Lindström 2015; Nechyporchuk et al. 2014; Karppinen et al. 2012). On the other hand, the parallel-plate configuration may lead to even more secondary effects when using too narrow a (below 1 mm) gap between the plates (Naderi and Lindström 2015; Nazari et al. 2016). These effects were not addressed beyond the dynamic critical stress (yield) point (i.e. in the linear viscoelastic regime; Cinar Ciftci et al. 2020; Schenker et al. 2018), as also confirmed by our preliminary study (Fig. S1). In addition, such a heterogeneous aggregate/flocculated network structure of MFC suspension was revealed to break gradually into smaller aggregates/flocs, or even disintegrate into eroding fibrils by increasing the shear rate (Saarikoski et al. 2012; Nechyporchuk et al. 2016; Koponen 2000). However, the effect of HEC/CMC addition to MFC could not be predicted, even from the course of the obtained stress dependent viscosity curves` profiles (Fig. S2). All of these phenomena were taken into account in this study, to evaluate the effect of HEC/CMC addition on the initial network structure of the 1.5 wt% MFC suspension by using a cone of very small (1°) angle and narrow truncation gap distance. Up to three repetitions were made, and an average measurement was taken; the typical Standard Deviations between the measurements were $\leq 10\%$. The noisy moduli data obtained at low strain values were omitted from the evaluation.

Rotational flow curve measurements were performed by increasing the shear rate continuously ($\gamma\cdot$) from 0.0001 to 1000 s^{-1} with 100 evenly distributed point measurements, obtained with an automated acquisition time mode (each of minimal 1.8 s) and shear rate control provided by the rheometer to prevent flow-instabilities, and, after reaching the maximum value, decreasing the shear rate directly, followed by the same interval (the whole CSR viscosity measurement requires approximately 6 min). The typically obtained flow curve (presented as viscosity, η in dependence of the shear rate, γ˙ vs. shear

stress, τ) from the increasing intervals was described by the zero-shear viscosity (η_0), the yield stress point (τ_y), and the power law parameters (consistency coefficient, K and flow index, N) according to the simple power law model ($\tau = K\gamma^{N-1}$) by fitting the curves as presented in Fig. 1a and illustrated in Fig. S3 for 1.5 wt% MFC (Schenker et al. 2019; Cinar Ciftci et al. 2020; Koponen 2000). As the exponents obtained from fitting the curves were rather sensitive to the distribution of data points, not necessarily

reflecting the true average behaviour of these suspensions accurately, and there were two yielding zones obtained in each η/τ dependency curve (also identified by other authors; Karppinen et al. 2012), the power law fitting for each zone was performed from the experimental data of the flow ($\eta(\dot{\gamma})$) curve (Figs. 1a and S1). The yield stress point (τ_y) was determined only in the first pass (as the cross-section of tangents applied to the zero-shear viscosity region and the first yielding region of the $\eta(\tau)$ curve), where

Fig. 1 Illustration of a fitting of **A** rotation and **B** oscillatory measurement curves of 1.5 wt% MFC suspension for describing its properties
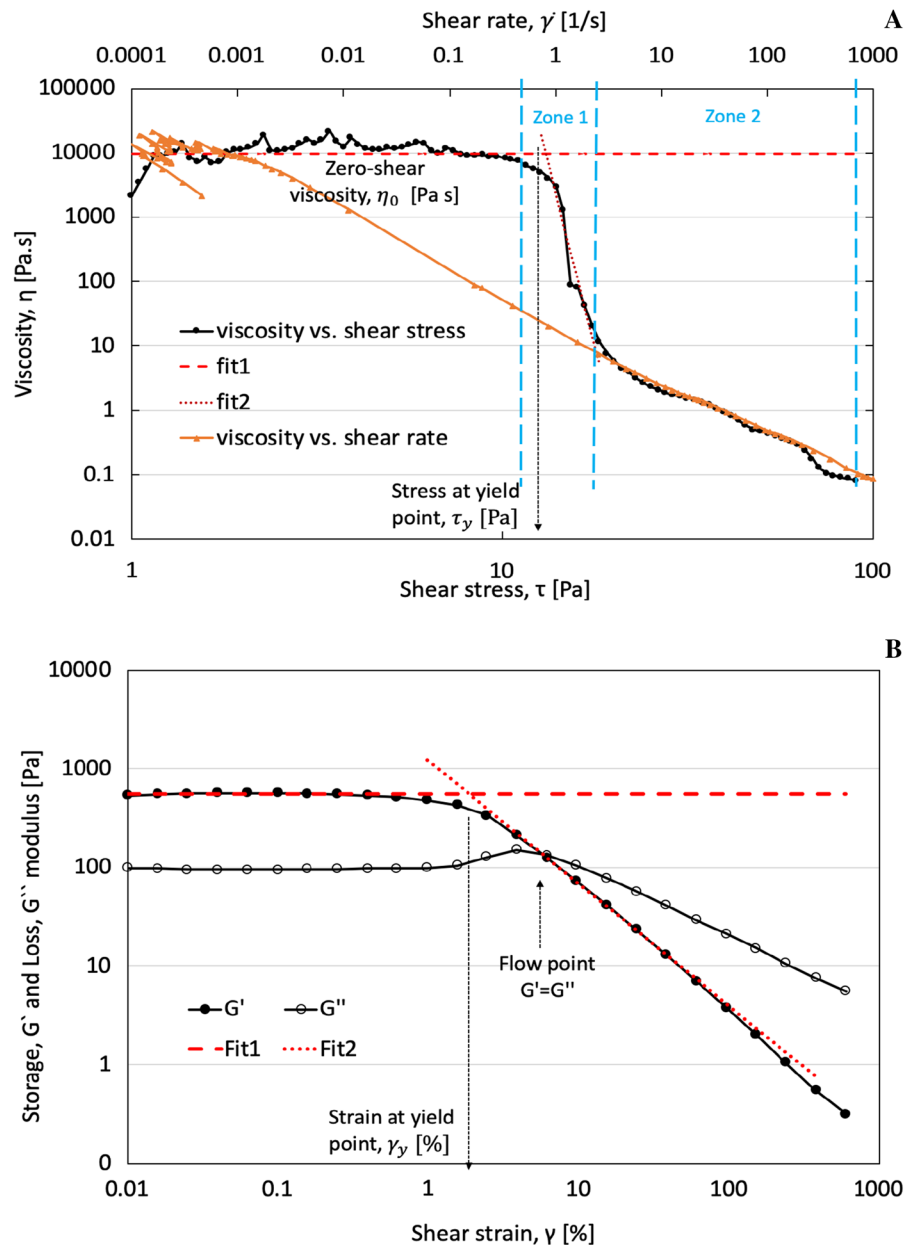
the viscosity decreased by several size classes with increasing shear rate. The zero-shear viscosity (η_0) was calculated as the average of all viscosity values obtained from $\eta(\tau)$ measurements at low shear stress, where the viscosity was constant. In addition, the hysteresis loop obtained from the shear rate increasing and decreasing curves is presented and described by giving the relevant viscosity values.

The viscoelastic properties were determined by an oscillatory amplitude sweep measurement at a constant frequency of oscillation (1 Hz = 6.28 rad/s) by increasing the shear strain (γ) from 0.01 to 600% with 25 evenly distributed point measurements of around 1.8 s acquisition time mode for all points. In addition, the frequency sweeps were performed in the frequency range from 0.01 Hz (0.062 rad/s) to 100 Hz (628 rad/s) at a constant shear strain ($\gamma = 0.1$–0.2%) within the Linear Viscoelastic Range (LVE) region determined by the strain amplitude sweep tests. The plateau values for the storage (G′) and loss (G″) modulus in the LVE regime (at 0.1–1% shear strain) were determined, as well as the yield points calculated fitting the G' curves from the tangential, as presented in Fig. 1b. The shear stress at which the value of G′ modulus dropped to around 90% of its initial value was defined as the yield stress. The tan δ (G″/G′) values and complex viscosities (η^*) were also calculated from the measurements described above.

Water retention properties

The water release of differently prepared MFC suspensions was measured with an ÅA-GWR (Åbo Akademi Gravimetric Water Retention Device, GRADEK). Before the measurement, the samples were diluted with water to a total solids content of 0.2 wt%. A known amount of the diluted sample (3 g) was filtrated through the membrane filter (nominal pore size 5 μm) for 30 s with 0.5 bar pressure, and the released water was collected and weighed. The results, the amount of released water from the amount of the sample (g/g), are given as an average of three measurements, and being recalculated in percentages.

Surface tension properties

The surface tension of both pure HEC/CMC solutions and differently prepared MFC suspensions were determined using a platinum Wilhelmy plate on a tensiometer (Krüss GmbH, Germany). The tested liquid (75 mL) in the vessel was placed on a movable table under the Wilhelmy plate. The plate was suspended vertically 6 mm into the tested suspensions, due to their relatively high viscosities. The surface tension (γ) correlates to the force (F) measured when the plate is pulled out, and was calculated by the Wilhelmy equation ($\gamma = F/(l \cdot \cos\varphi)$, where l is the wetted perimeter (2w + 2d), w is the plate width, d is the plate thickness, and φ is the Contact Angle (CA) between the liquid and the platinum plate). The average values were calculated from at least four individual measurements.

Results and discussion

Microstructure of MFC suspensions

The microstructure of the water-suspended MFC was quantified with SEM imaging. It is manifested clearly from Fig. 2, that the pure MFC suspension is highly polydispersed, containing larger fibril fragments of approximately up to 50 nm in diameter, and the length of a few μm, surrounded with more or less delaminated thinner fibrils. These fibrils are attached to one another tightly (are overlapping each other significantly) due to physical attractions originating from the surface OH-group mediated hydrogen bonds and van der Waals interactions (Kuijk et al. 2013), forming a complex, highly entangled, web-like network structure of differently large segments (less and smaller voids, as well as bundles of fibrils), and also the presence of slightly agglomerated/flocculated structures. The addition of 20 w/w% of relatively highly-M_W HEC2 (700.000 mol/g) and HEC3 (1.300.000 mol/g) did not affect the dispersibility of the cellulose microfibrils or their deagglomeration, but resulted in a more dense structure with relatively good integrated HEC polymers. This effect was even more pronounced in the case of using CMC4 ($M_W = 700.000$ g/mol) at even much lower content (5 w/w%), which might be related to a higher swelling ability of those polymers due to the presence of carboxylic groups (DS = 0.8–0.95) on their backbones.

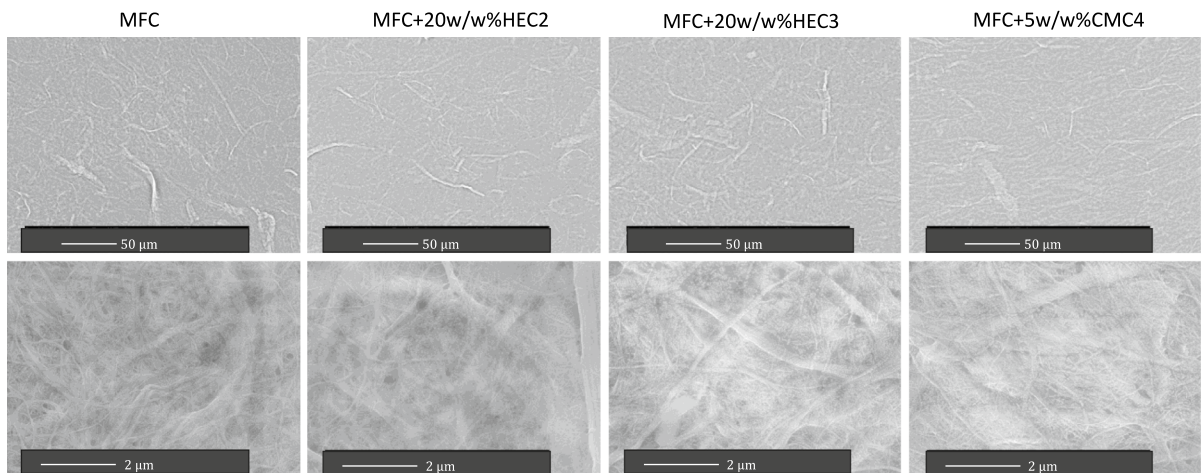| MFC | MFC+20w/w%HEC2 | MFC+20w/w%HEC3 | MFC+5w/w%CMC4 |

Fig. 2 SEM images of MFC-based suspensions obtained at different magnifications

Rotational tests: flow behaviour

The viscosity (η) versus shear rate ($\dot{\gamma}$) curves (obtained by the controlled shear stress approach where the shear rate is measured) of MFC suspensions, with and without the addition of 20 w/w% HECs or 5 w/w% CMCs (as representative concentrations), are presented in Fig. 3a. In general, all the MFC suspensions exhibited a highly viscous structure at low shear-rates conditions and a shear-thinning behaviour (i.e. decreasing of the viscosity with an increased shear rate). All curves also show a faster change of the structure in the shear rate region between 0.01 and 1 s^{-1} given by the rather limited number of measuring points, probably due to insufficient time for contact points between the still flocculated fibrils to get stabilised. The shear-rate and time-dependent behaviour of the hysteresis can also be observed, whose unconnected loop in the reverse shear rate between 0.1 and 100 s^{-1} appears to move to the left (to the lower shear rates) in the graph, and become weaker upon the addition of certain HEC/CMCs, corresponding to the larger shear stress which occured in such MFC-based suspensions in that region. This could mean that the initial fibrillar flocculated network of MFC suspension changes its structure by reorganisation in a way to be less susceptible to the higher shear rates. However, bearing in mind the relatively narrow truncation gap distance between the cone and plate which were used during the measurements, and the fact that the floc size is inversely proportional to the shear rate and dependent on the geometry gap (Saarikoski et al. 2012), this could, in addition, not only limit the detection of the largest fibrillar flocs, but might also remove them from a certain distance around the geometry boundary, leaving a layer of low viscosity suspension with smaller, and in the flow direction, rearranged flocs, and/or individual fibrils eroding from them in the measuring place. In addition, while certain MFC suspensions containing HEC/CMCs show no viscosity measurement points at higher shear rates (100–1000 s^{-1}), this might therefore mean that the fibrillated structures formed in the presence of HEC/CMC were larger and thicker, and, thus, unable to adapt physically to the narrow gap distance under faster shear rates, and were therefore removed from the measuring geometry at those shear rates. On the other hand, higher shear rates might also cause irreversible changes (aggregation) to such suspension`s network structures.

The share rates yielded different stresses to such structured MFC-based suspensions, as is evident from their shear stress (τ) dependent viscosity (η) curves, presented in Fig. 3b. All these curves have a similar profile, where the viscosity is constant at low shear stresses, and it falls significantly above a certain threshold of the shear stress (corresponding to the 1st yield region, Fig. 1) due to the decomposition/reorganisation of the larger fibril aggregates and floccules, followed by another, much less pronounced and more continuous decrease (corresponding to the 2nd yield region), with a further
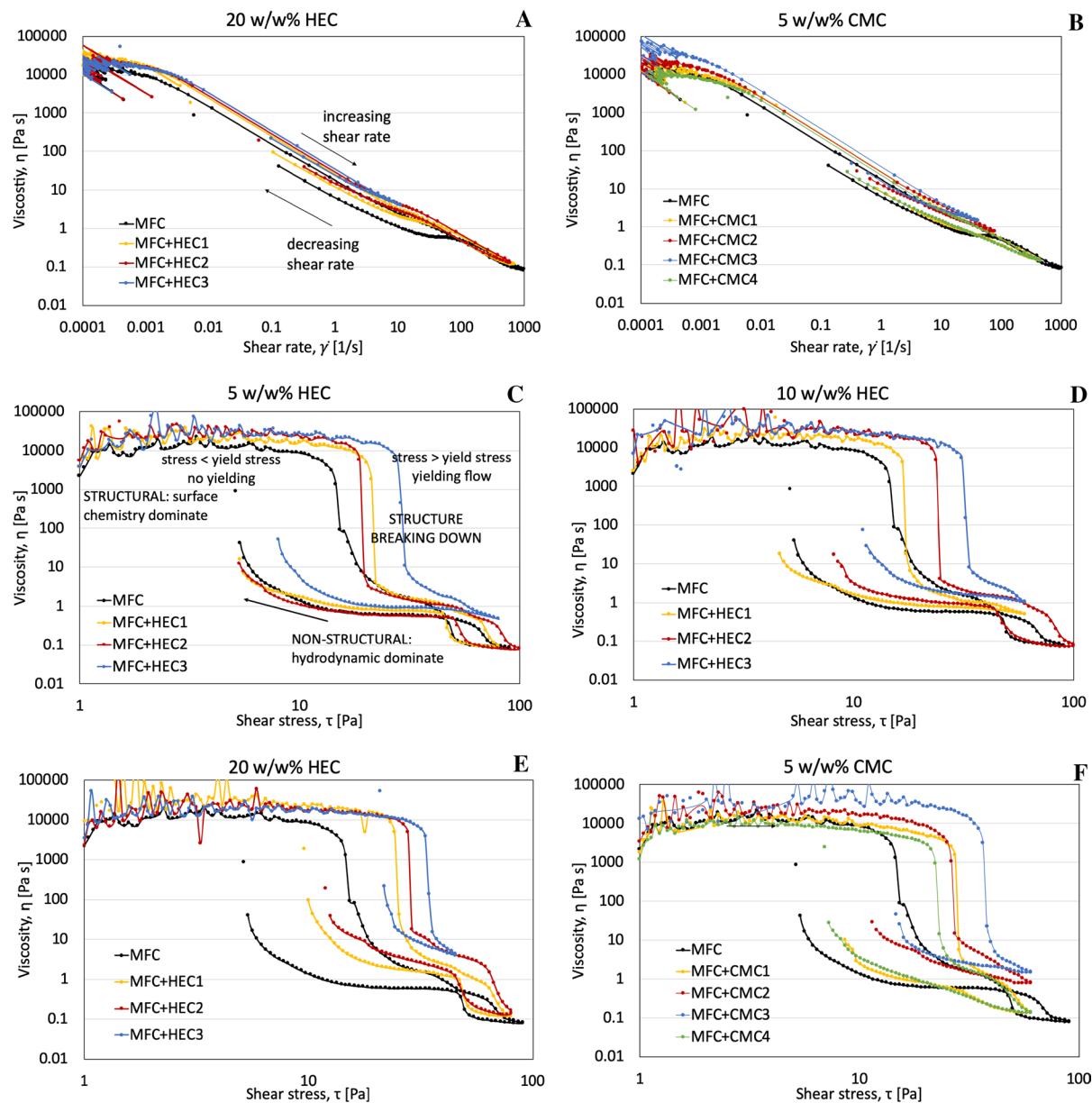
Fig. 3 **A**, **B** Shear rate and **C–F** shear stress dependent viscosity curves for 1.5 wt% MFC suspension with and without the addition of **C** 5, **D** 10, and **A**, **E** 20 w/w% HEC of different M_W and **B**, **F** 5 w/w% CMC of different M_W and DS, respectively. Legend: MFC (without HEC/MFC, black line), MFC with HEC1 or CMC1 (yellow line), MFC with HEC2 or CMC2 (red line), MFC with HEC3 or MFC3 (blue line), MFC with CMC4 (green line)

increase of the shear stress. These suspensions also have different high viscosities at low shear stresses, the plateaus of which are destroyed at different shear stresses, depending on the addition of HEC/MFC, that, consequently, affect their behaviour at higher shear rates/stresses.

The zero shear viscosity (η_0), determined from $\eta(\tau)$ measurements at low shear stresses, where the viscosity was constant (Fig. 1), revealed that the pure MFC suspension exhibited the lowest η_0 ($\approx$11 kPa s), which was increasing with the addition of HEC and increasing of HEC' M_W (Fig. 4) in accordance with
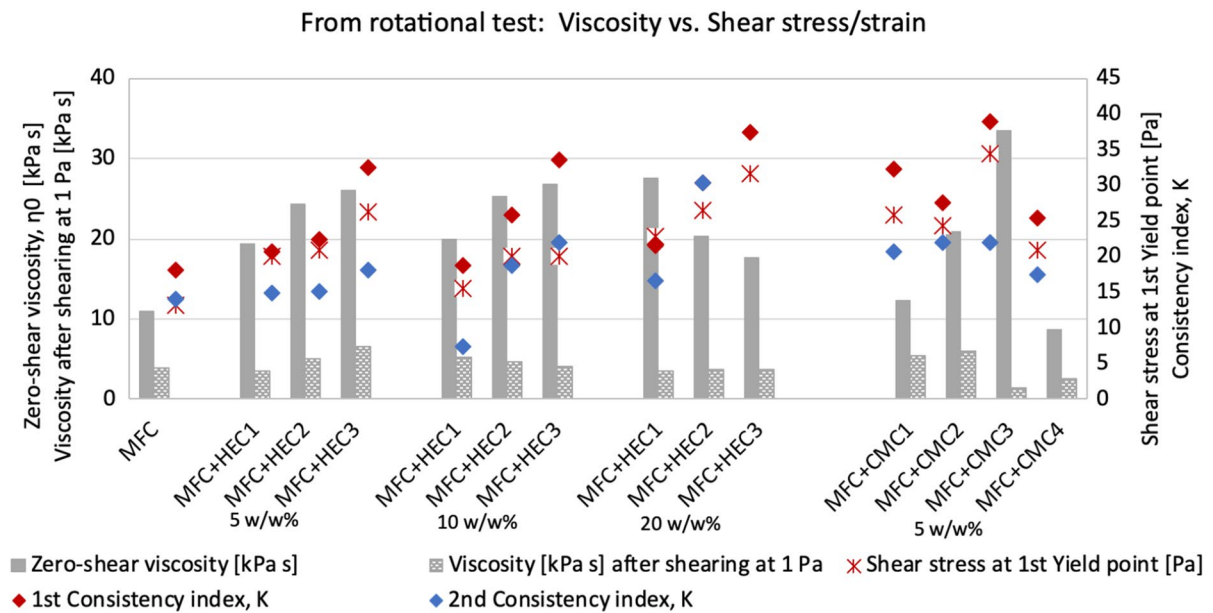
Fig. 4 Zero-shear viscosity (η_0) and Yield point (τ_y) values with relevant consistency (K) and flow behaviour (N) index parameters, as well as viscosity after shearing (at 1 Pa in a decreasing shear loop) of 1.5 wt% MFC suspension with and without the addition of (5, 10, and 20 w/w%) HEC of different M_W or (5 w/w%) CMC of different M_W and DS, respectively. All data are presented in Table S1

the polymer theory (Sviderskyi et al. 2018). Anyway, this was valid only for 5 w/w% and 10 w/w% of HEC addition, while, with its higher (20 w/w%) content, the η_0 was additionally increased only for the suspension containing the lowest M_W HEC (HEC1 of 90.000 g/mol, to ≈27.5 kPa s), while it was decreased for samples prepared with HEC2 and HEC3, among which the suspension containing the highly M_W HEC (HEC3 of 1.300.000 g/mol) resulted in the lowest η_0 (≈17.6 kPa s) among all of them. The viscosity of the MFC suspension at low shear stress was also found to fluctuate notably in the logarithmic scale, probably due to the formation of relatively unhomogeneous (differently large, stiff and strong) aggregated/flocculated fibrils` networks, as being evidenced from the SEM images (Karppinen et al. 2012; Cinar Ciftci et al. 2020; Schenker et al. 2019) with reduced mobility. This effect was even more pronounced in the case of adding HEC to the MFC suspension, whose varying viscosities in this region indicate the in/ability of HEC to become integrated homogeneously within the initially formed aggregated/flocculated network structures of fibrils. Furthermore, HEC polymers could probably not disintegrate some more intertwined and

strongly interacted flocks of fibrils, or they become structured in new, larger and stronger bands (Dimic-Misic et al. 2013b) while forming weaker structures with freely suspended fibrils in between. The described structures can, thus, lead to the formation of intra-structural regions of different viscosities, and, thus, flow properties, which, when having in mind the differently large, stiff and interfibrillary-interacting nature of the hybrided MFC/HEC structures, also act as a precursor for their transformation at higher shear stresses (Nechyporchuk et al. 2014).

At a certain shear stress the viscosity decreased until a first plateau was reached (at about $\tau > 10$ Pa), being a consequence of the progressive structural deformation of the MFC network, where fibrils agglomerates/floccules started to de-agglomerate/flocculate, or larger structures being squeezed from the measuring geometry at those shear rates due to the problems described above, being, however, expressed by the 1st yield point. The samples with higher yield points were, thus, able to resist higher stress, because the strength of the fibrillated network structure was higher, and, thus, more force was needed to change the structure of such suspensions. The yield point of the

pure MFC suspensions (which occurred at $\tau \approx 13$ Pa) thus increased with increasing the M_W of the added HEC, reaching the highest value ($\tau \approx 23$–31 Pa) for the suspension with addition of the highest M_W HEC (HEC3 with $M_W = 1.300.000$ g/mol). The flow behaviour index (N) corresponds to the changing of such structures, thus, varying/decreasing from about 0.055 for pure MFC to about 0.021–0.045 as a function of the solid content and M_W of HEC increasing, while the consistency index (K) was increased proportionally (from around 18.12 for pure MFC to around 18.76–38.86 for the hybrid with HEC polymers). By increasing the shear stress further a 2nd yielding zone could be observed at around $\tau > 40$ Pa, indicating additional fibril's de-agglomeration/flocculation (probably destroying parts of—in the measuring gap remaining—smaller, stiffer and strongly intertwined fibrils), given also the maximum organisation (more aligned planar structures) of the fibrils in suspension in the tested shear stress range. The addition of HEC was making the 2nd yielding zones less pronounced and shortened, the maximum value of which was shifted to the lower shear stress (Table inserted in Fig. 4) by increasing the HEC's M_W and concentration, i.e. from around 22–90 Pa for pure MFC to around 38—60 Pa for MFC containing 5–10 w/w% HEC3 of 1.300.000 g/mol, given the viscosities between 5 and 15 Pa s. The flow indexes increased accordingly to around 0.16–0.45 (and the consistency indexes generally reduced to around 7.31–30.39), depending on the network`s structure formed after the 1st yielding zone and their additional changing during the higher shearing. The HEC3 with the highest M_W had a greater structure forming effect (Sviderskyi et al. 2018), and, thus, provided the well-defined pseudoplastic properties of the MFC suspension, the 2nd yielding of which could not be evaluated. Such behaviour can be attributed to both the earlier/faster (at lower shear stress) alignment of individual fibrils (still remaining in the measuring gap, and, in the flow direction oriented smaller, more densely packed and rigid fragments of the remaining agglomerated/flocculated fibrils hybrided with the HEC under shearing, by forming cylindrical structures, as compared to the pure MFC suspension, thus all together resulting in viscosity dissipation and slippage of such less viscous suspensions (Karppinen et al. 2012). After reaching the maximum value and shear stress decreasing, the MFC suspensions followed a similar trend in the

feedback loop, although they returned to different viscosities and differently high shear stresses, depending on the HEC addition. The fastest recovery was, thus, obtained for MFC containing 20 w/w% of HEC3 (at ≈ 20 Pa), yielding the highest viscosity (≈ 5.24 kPa s). Although the structures formed during the shearing were not returned completely to the previous/initial state formations, their reversibility profiles give rise to better understanding of their changes under higher shear speeds and loadings.

In comparison, the flow behaviour of MFC suspensions containing 5 w/w% of CMC with different M_W and DS (Figs. 3, 4) gave the highest zero shear viscosity (η_0) for CMC3 (≈ 33.3 kPa·s) with the highest DS (DS = 1.2), while it was reduced to around 20 kPa·s for CMC2 with similar M_W (250.000 g/mol) and lower DS (DS = 0.8–0.9), and decreased further by the addition of CMC1 (to ≈ 12.2 kPa s) and CMC4 (to ≈ 8.7 kPa·s) with similar DS (DS = 0.7–0.85) but different M_W (90.000–700.000 g/mol). It is also obvious that a decrease of the viscosity in the 1st yielding zone occurred at the highest shear stress (≈ 35 Pa) for the suspension containing CMC3, and it was sharper compared to the MFC suspensions containing HEC (which occurred at ≈ 15–31 Pa) or CMC with lower DSs (DS < 1.2, which occurred at ≈ 20–26 Pa). The 2nd yielding zone was, generally, additionally reduced (to 26–60 Pa), given an irreversible (after reduction of the stress) viscosity profile at much higher shear stress (at around 15 Pa, thus yielding viscosity of around 49 Pa s at the last point at which it was measured), which indicated the best fibrils` integration with the surface charged CMC ($K_{1st} \approx 25.39$–32.26, $K_{2nd} \approx 17.43$–21.99), as well as their flowing ($N_{1st} \approx 0.024$–0.045 and $N_{2nd} \approx 0.18$–0.27) and stability after relaxation. This trend, although much less pronounced, was reduced primarily with the addition of a lower M_W CMC, and secondly with its lower DS, i.e. from CMC3 to CMC2, followed by CMC1 and CMC4, the latter also giving a much wider shear stress hysteresis. Such flow behaviour of MFC/CMC-based suspensions support the previous findings on the formation of generally larger and also more flexible aggregated/flocculated fibrils` structures in suspensions containing CMC by their better dispersibility (due to the surface adsorbed CMC, Butchosa and Zhou 2014) reducing the friction, and, thus, the rigidity between them, and allowing their easier movement and orientation upon the

application of shear. The results also coincide with other studies, where it was found that the flexibility of low surface charge cellulose fibrils is directly dependent on the fibrils` size distribution (Cinar Ciftci et al. 2020), and, as such, contributes importantly to their rheological behaviour, above all, beyond the yield point (Ishii et al. 2011; Butchosa and Zhou 2014), i.e. at flow initiation. Such flexible behaviour might also be related to the higher swelling ability of CMCs (due to the presence of the carboxylic groups), as well as their repulsive interactions with the rare negative surface charge groups present on the MFC (given a zeta potential of around 28 mV in a pH of 6.5, Karim et al. 2019), that contribute to the depleting of fibrils at the solid boundaries of simple shear flow. On the other hand, good adhesion of CMC to the fibrils, due to hydrophobic interactions arising from the non-polar methyl moieties at CMCs, can increase their networking (Medronho et al. 2012).

It is obvious that the cellulose polymers (HEC/CMC) can hold cellulose fibrils apart from each other, thereby delaying contact and diminishing the development of frictional forces, thus affecting rheological behaviour significantly. Under static or low shear conditions, beyond the yield point, the presence of HEC/CMC can, thus, exhibit diverse rheological behaviour, depending on the surface charge and hydrophobicity of the solids (both HEC/CMC and MFC) and their water binding properties. In the case of MFC, the application of strain under low shear for continued periods can lead to structure ensemble orientation. The strong mutual electrostatic repulsion of the highly charged CMC and the immobilisation of the trapped interstitial water, act together to create highly elastic structured zones that are manifested as a time-dependent increase in viscosity (Dimic-Misic et al. 2013a). When such suspensions are exposed to an increasing ultralow shearing (in the zero-shear viscosity region), the developed fibrils and fibrils with integrated HEC vs. CMC complex structures arising from the MFCs initial aggregation/flocculation and the ability of HEC/CMC to interact with them and integrate, can lead to the formation of intrastructural regions of different viscosities (due to the formation of differently-large fibrils` floccules with/without integrated HEC/CMC, also dispersed optionally in between the water-rich and differently large HEC/CMC polymer clusters; Schenker et al. 2019). It can also be proposed that smaller clusters become

structured into larger under the prolonged influence of low shear below the yield point (Dimic-Misic et al. 2018). The flow properties are, thus, rendered primarily by the integrated water-binding HEC/CMC, leading to fibrils` clusters` alignment (formation of more entangled structures) at higher shearing, and depending on the solids` charge and aspect ratio of fibrils vs. HEC/CMC dominating the flow curve. Swelling of both MFC and HEC/MFC can also reduce the friction between fibrils in a suspension, thus allowing fibrils` movement upon the application of shear. CMCs that have a higher surface charge and are generally more water-swollen and flexible than low-charged HECs, can, therefore, create less friction at low shear, while, under higher shearing conditions, they exhibit more pronounced decreases in viscosity as a consequence of flow (Dimic-Misic et al. 2013a). The shear-thinning effect is, thus, more pronounced, and the onset of shear-thinning generally starts at lower applied shear stresses (Fig. 3).

The breakdown and recovery of suspensions can also be described by thixotropic shear-thinning behaviour. As seen from Fig. 5, an increase of shear rate results in a deformation and flow curves showing hysteresis loop and thixotropic behaviour (returns to a point similar or a bit lower than the initial critical shear stress), being governed by a hydrodynamic shear stress that distorts or pulls aggregations/floccules and fragmentation of MFC vs. MFC containing HEC/CMC suspensions` structures apart. The area within the hysteresis loop thus represents the energy consumed in the structure`s breakdown, indicating the extent of the thixotropy, which was significantly lower in the case of the addition of high-M_W HEC (HEC3), and even less pronounced in the presence of medium-M_W CMCs of higher DS (CMC2 and CMC3). The addition of HEC/CMCs might thus reduce the hydrogen bonding interactions between cellulose microfibrils, resulting in less dense and physically weaker aggregates and fibrils` bundles in such a mixtured suspension by localised integration, which improves fibrils` distribution, and, hence, increases their mobility in such a network.

Oscillatory testing: amplitude sweep (viscoelastic behaviour)

Oscillatory measurements are used to examine the contributions of solid-like (elastic) and liquid-like
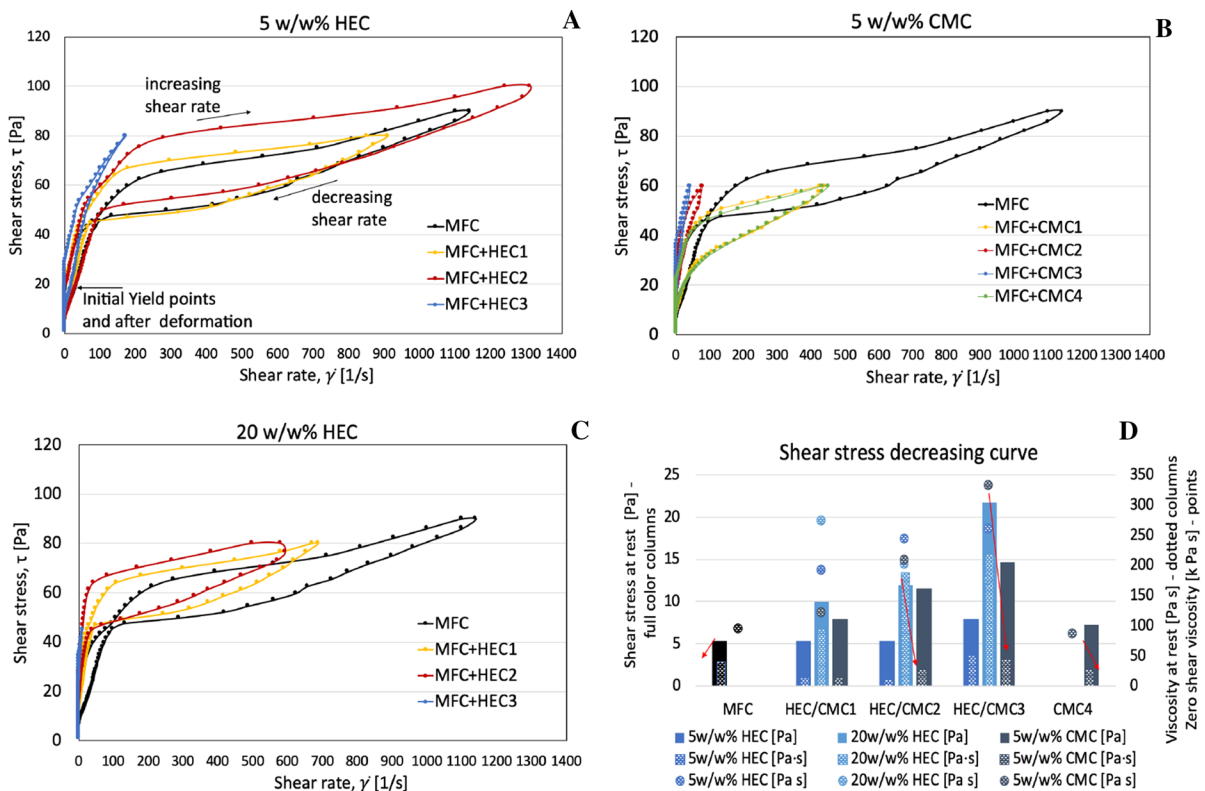
Fig. 5 Thixotropy of 1.5 wt% MFC suspension with and without the addition of **A** 5 and **B** 20 w/w% HEC of different M_W or **C** 5 w/w% CMC of different M_W and DS, respectively, at different increasing/decreasing shear stress/rate measuring profiles, with corresponding **D** viscosities before (zero-shear) and after applied shear stresses. The legend for the coloured lines of the rheological measurements correspond to the description in Fig. 3

(viscous) interactions to the flow characteristics and mechanical properties of suspensions. The MFC-based suspensions were, thus, subjected to an increasing oscillating strain at a constant frequency (amplitude sweep), or vice versa (frequency sweep), to determine their viscoelastic behaviours, where the obtained elastic modulus (G') describes the solid-like, whereas the loss modulus (G") defines their liquid-like behaviours. As already examined well by other researchers (Cinar Ciftci et al. 2020; Pääkkönen et al. 2016), and can be verified from Fig. 6, all MFC-based suspensions possess a linear response at low shear stresses (in the Linear Viscoelastic Regime/ LVE), wherein both G' and G" are independent of the shear strain, and G' is dominant over G", indicating that the suspensions are acting consistently solid-like by forming a differently strong fibrillar network. At a critical shear strain (at about 2%), the suspensions start to yield, being shown by a decrease in G',

and then reach a crossover or flow point where G" becomes dominant (G" > G') and the sample begins to flow, indicating that the fibrillar network structures have broken down and begun to behave as a non-Newtonian shear-thinning fluid. The shear stress of the equilibrium modulus (G' = G") for the pure MFC suspension was determined to be around 11 Pa, resulting in a deformation or shear strain of around 5.8% (Fig. 7). The flow point values of MFC suspensions containing HEC are increased by modulus (from tan δ ≈ 0.57 up to ≈ 0.20) and shifted to higher shear strains (up to 9.2%) by increasing of HEC' M_W, resulting in up to ≈22 Pa of the shear stresses for an MFC suspension containing 20 w/w% of the highly M_W HEC (HEC3 of 1.300.000 mol/g). For MFC suspensions containing 5 w/w% CMCs, already the yielding is shifted to the higher shear strains (to ≈ 4.5% from ≈1.84% at pure MFC or ≈1.4–3.7% for MFC/HEC suspensions) due to the slower
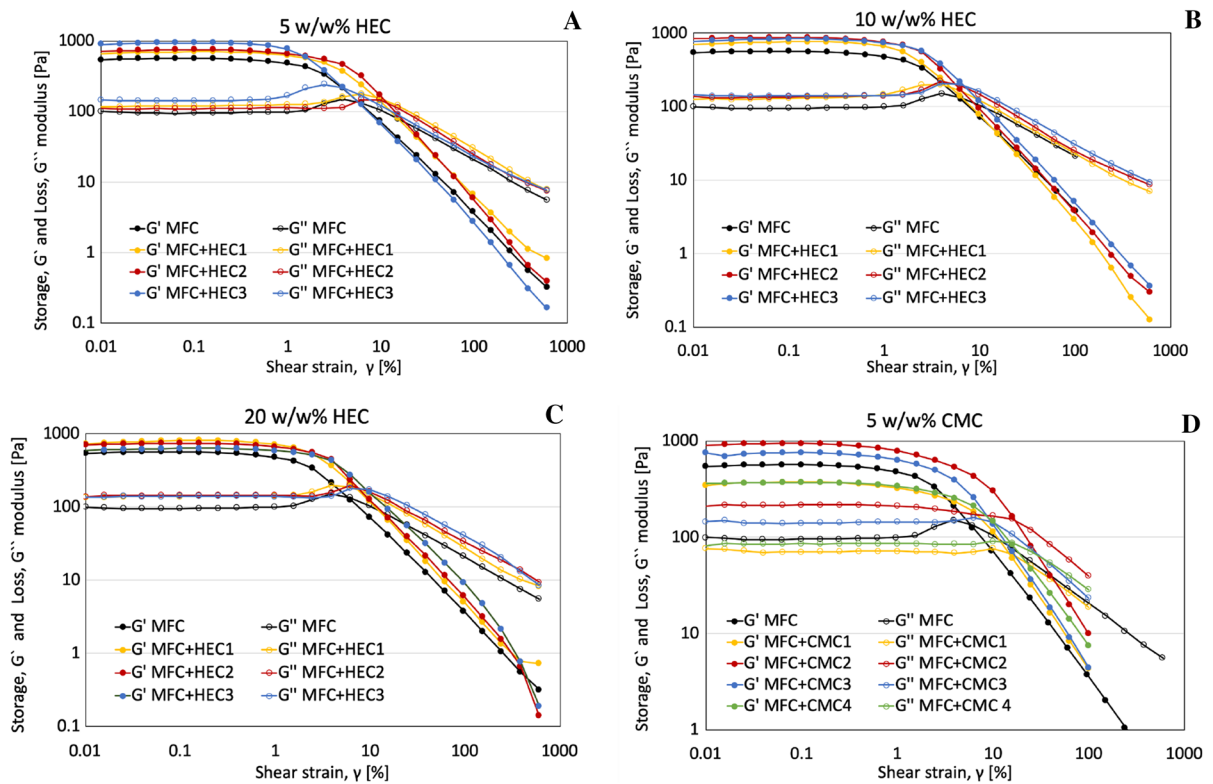
Fig. 6 Oscillatory amplitude tests at constant frequency (1 Hz) for an MFC suspension with and without the addition of **A** 5, **B** 10 and **C** 20 w/w% HEC of different M_W and **D** 5 w/w% CMC of different M_W and DS, respectively. The legend for the coloured lines of the rheological measurements corresponds to the description in Fig. 3

deformation process for those suspensions, except the suspension containing CMC3 with the highest DS (DS = 1.2, ≈3.1%), and the region between yielding and flow extended as compared to all other MFC/HEC suspensions. The cross-over points of modulus thus appeared at significantly higher shear strains (15–17%). Such a behaviour of those suspensions confirmed the generally stronger network structures (being also expressed in lower complex viscosities), among which the the MFC suspensions containing CMC2 (M_W = 250.000 g/mol, DS = 0.8–0.9) and CMC4 (M_W = 700.000 g/mol, DS = 0.8–0.9) were the strongest, followed by the one containing CMC1 (M_W = 90.000 g/mol, DS = 0.7), while it was reduced to around 10% for the suspension containing CMC3 with relatively low M_W (M_W = 250.000 g/mol) but the highest DS (DS = 1.2). Such properties of MFC/CMC suspensions could also be related to the better water retention properties of highly water-binding CMC, as already established by Pääkkönen et al. (2016).

This also indicates that the applied strain used for the processing of those MFC/CMC-based suspensions could be higher without completely destroying their structure.

Oscillatory testing: frequency sweep

The frequency tests were performed at constant deformation (0.1–0.2%) within the linear viscoelastic range, and varying the frequency of oscillation from f = 0.01–100 Hz (Fig. 8). For all samples, complex viscosity decreased with increasing frequency in the same manner for different HEC or CMC additives. All MFC-based dispersions also exhibited solid-like behaviour, with G′ > G″ over the entire examined frequency. Both moduli increased with increasing the frequency, indicating that the network structure formed by the microfibrils was in the dynamic mode of physically formed entanglements, resulting in a stable gel-like behaviour. However, the modulus for
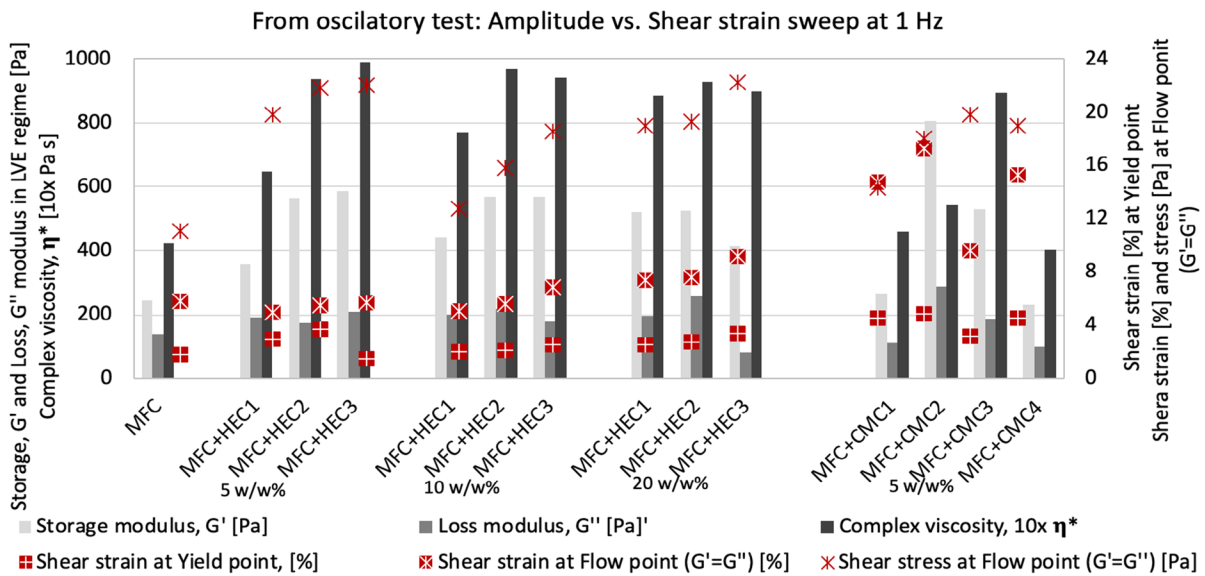
Fig. 7 The dependency of the addition of (5, 10 and 20 w/w%) HEC of different M_W and (5 w/w%) CMC of different M_W and DS, respectively, on the rheological parameters of 1.5 wt% MFC suspension, determined by oscillatory testing at constant strain/deformation (0.1–0.2%) and frequency (1 Hz = 1 s^{-1}). All data are presented in Table S2

MFC suspensions containing HEC showed noticeably higher values for both parameters and in the whole measuring range, which depended on the type and concentration of HEC added, indicating differently strong/stiff agglomeration/floccules' networking structures formed with fibrils. This was also reflected in a change of their complex viscosity (an increase from about 4250 Pa s for pure MFC up to about 9700 Pa s for MFC containing HEC; Fig. 7), measured at 0.2% strain and 1 Hz frequency, additionally confirming the formation of differently strong clusters of MFC/HEC vs. CMCs, that modulate the height of the complex viscosity, as well as the G′ and G″ modulus. Similar viscoelastic behaviour was observed with aqueous suspensions of MFC containing CMC (Agarwal et al. 2018), or other polymeric additives such as pectin (Agoda-Tandjawa et al. 2012).

It was also possible to observe some divergence in the rheological behaviour of MFC/HEC suspensions compared to MFC/CMC ones with similar solid content (5 w/w %). This may be related primarily to the higher surface potential of highly carboxylated CMC compared with HEC, and, secondly, with their M_W. CMC would form larger and more open cluster structures compared to the HEC of similar M_W, bearing only OH surface groups, resulting in huge H-bonding

and highly conformed smaller /denser networks, and, thus, higher zero-shear viscosities of higher flow points (shear stress) and more dynamic (G′ and G″) rheological properties. It is obvious that the addition of a higher HEC concentration to MFC suspensions does not modify their viscoelastic and microstructural properties significantly, and the mixtures are controlled mainly by the cellulose fibrils. On the other hand, an increased viscosity with an increased ionic strength of CMC, leading to a higher electrostatic repulsive force between them, and, thus, also to a different form of fibrils` interaction, which forces, however, collapse at higher shear stress (i.e. higher strength is needed to decrease such a gel`s strength structure) compared to a pure MFC-based one.

The tan δ values (which represent the ratio between G″ and G′) have been used to describe the viscoelastic response of the suspensions at different viscoelastic regions, and, thus, to predict their strength. Figure 9 shows that the values of tan δ obtained at low frequency (f = 0.025 Hz, in LVR) and at the yield point, and plotted against an increasing proportion of HEC/CMC in the MFC suspension, primarily decrease with increasing the M_W of the HEC, and secondly with increasing of its concentration, and with the increasing DS of the CMC. Although those values
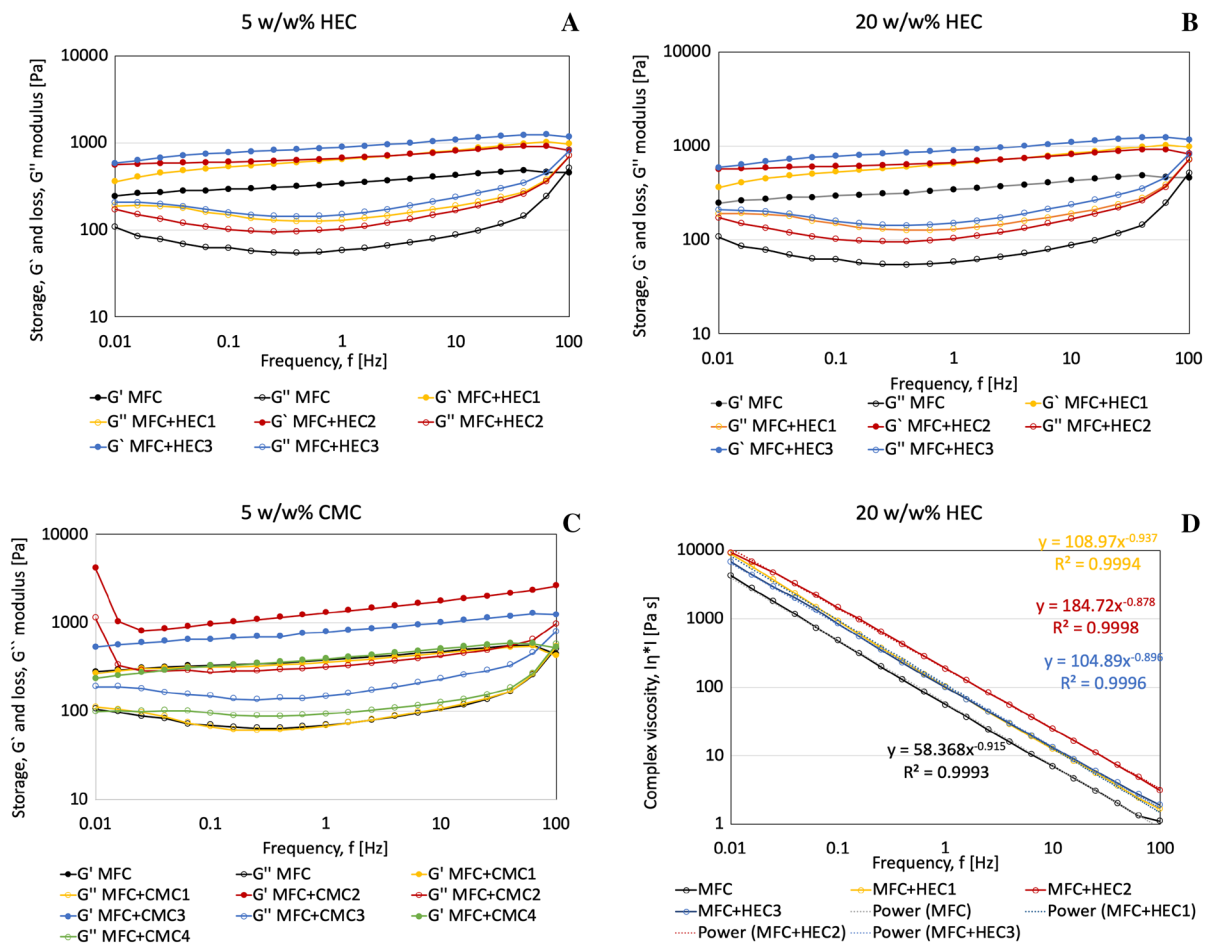
Fig. 8 Oscillatory frequency tests, performed in a linear viscoelastic range at constant strain, and its complex viscosity for 1.5 wt% MFC dispersions with and without the addition of **A** 5 and **B** 20 w/w% HEC of different M_W, **C** 5 w/w% CMC of different M_W and DS, and **D** corresponding complex viscosities for 1.5 wt% MFC dispersions with and without the addition of 20 w/w% HEC of different M_w. The legend for the coloured lines of the rheological measurements corresponds to the description in Fig. 3

were much higher when reaching the yield points, the trends were similar, additionally confirming the formation of differently strong network microstructures.

Water retention and surface tension properties

The water retention and surface tension properties of selected MFC-based suspensions were determined in addition, to assess/confirm their contribution/impact on the rheological properties, above all, the zero-shear viscosity, flow properties and structural recovery after elastic deformation. As shown in Fig. 10, the addition of both CMC or HEC to the MFC suspension obviously improved its water retention properties.

The water removal values of MFC-based suspensions were, thus, reduced from about 70% to 25–35% by the addition of HEC or CMC, which order—from the highest to the lowest values for the samples analysed—was HEC1 ($M_W = 90.000$ g/mol) > HEC3 ($M_W = 1.300.000$ g/mol) > CMC3 ($M_W = 250.000$ g/mol, DS = 1.2) > CMC4 ($M_W = 700.000$ g/mol, DS = 0.8–0.95). This indicates that the carboxylation degree (DS) of CMC has a higher effect on the water retention of MFC-based suspensions than that of its Mw. The higher waterretention of CMC-based polymers is related to the better accessible carboxyl and hydroxyl groups available for hydrogen bonding with water molecules, which can, in combination

Fig. 9 Values of Tan δ in the linear viscoelastic region (LVR) at f = 0.025 Hz and at the Yield point obtained from the frequency test
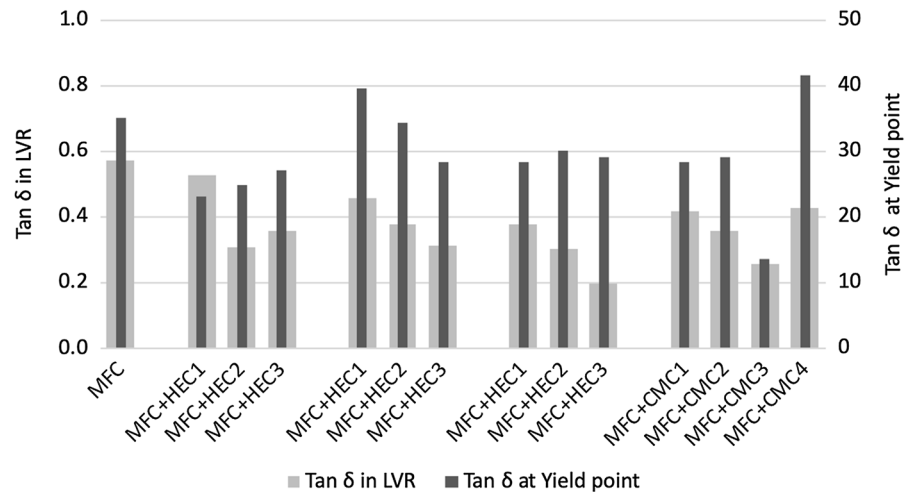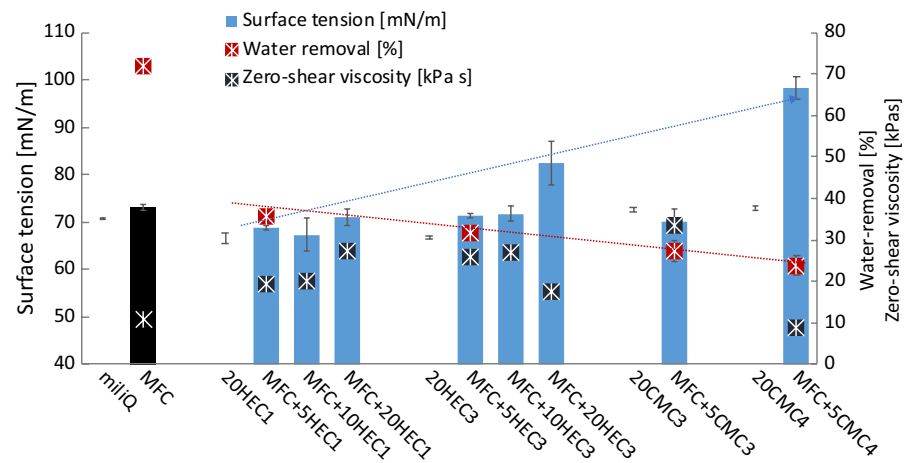

Fig. 10 Water-removal and surface tension properties of different HEC/CMC solutions and corresponding MFC-based suspensions, respectively, with respect to their zero-shear viscosities

with a higher degree of MFC de-aggregation/flocculation, increase the fibrils' surface area and amount of CMC/HEC integration between the fibrils, thus forming larger, more dense and stronger cluster-based network structures, as confirmed by the rheological measurements.

The surface tension of a polymeric suspension is also an important parameter, affecting its dispersibility and physical stability, while reducing its viscosity (Ahmari and Amiri 2015). The pure HEC solutions exhibited negligible surface activity, which surface tension was slightly lower (≈67 mN/m) or close to that of milli Q water (≈70 mN/m), independent of the HEC's M_W. On the other hand, the surface tension of pure CMC solutions was slightly increased (≈72 mN/m) similar to that of the pure MFC suspension

(≈73 mN/m) with negative surface charge. Although the Wilhelmy plate method, which was used in this study to measure the surface tension, might be affected by the viscous force arising from the surface detachment between the plate and the viscous liquid, thus resulting in its increases (Lee et al. 2012), the surface tension data trend was obviously affected by the SD of the CMC and its Mw, i.e., an increased surface polarity of the cellulose polymers (the presence of surface-active carboxylic groups) that enhance the interfacial interaction, and, thus, affect the stacking density and distribution of the hydrophilic and hydrophobic segments of the cellulose chain (Miller and Donald 2002) in the MFC suspension. The surface tension of the pure MFC suspension was, thus, increased additionally to ≈98 mN/m with the addition

of 5 w/w% of highly DS' CMC4 ($M_W = 700.000$ g/mol, DS = 0.8–0.95) and slightly (~82 mN/m) with 20 w/w% of highly M_W HEC3 ($M_W = 1.300.000$ g/mol). At the same time, its zero-shear viscosity was reduced from ≈33–17 kPa s to ≈8.7 kPa s, which indicates a comparatively more stable and less aggregated suspension due to the repulsive interactions between the negatively charged carboxylic groups, followed by MFC suspensions with 20 w/w% of HEC1 ($M_W = 90.000$ g/mol) and 5 w/w% of CMC3 ($M_W = 720.000$ g/mol).

Conclusion

In the present study, the rheological behaviour of highly-branched (flocculated) and polydispersed 1.5 wt% microfibrillated cellulose (MFC) suspensions have been investigated after the addition of various amounts (5–10–20 w/w%) of water-soluble hydroxyethyl (HEC) and carboxymethyl (CMC) celluloses of different molecular weights ($M_W = 90.000–130.0000$ g/mol) and degrees of substitution (DS = 0.7–1.2) by performing steady shear rotational (viscosity vs. shear rate) and oscillatory (viscoelastic) flow in amplitude and frequency sweep tests using cone-plate measuring geometry. It was shown that, already, the addition of a very low (5 w/w%) concentration of high-M_W HEC or middle-M_W CMC with high DS, improved the colloidal dispersibility of the fibrils and their flocculated structures, giving a higher and stability-prolonged zero-shear viscosity with a more linearly decreased viscosity profile (shear-thinning behaviour) by reducing, or even eliminating, the second yielding zone, that was otherwise obtained with the pure MFC suspension, due to the reduced effect of fibrils` agglomeration and/or flocculation. In addition, due to the higher water retention ability of such HEC/CMC, they yielded MFC suspensions with higher surface tension properties, and, thus, stronger microstructures, that can be processed at higher shear rates or stresses, given the almost irreversible and faster viscosity rebuilding after stress reduction. The MFC/CMC suspensions also possessed a wider linear viscoelastic region with the flow point at higher shear stress, although they revealed a stronger decrease of complex viscosity with increasing frequencies, due to the formation of a more stable and viscoelastic gel-like structure with significantly higher elastic contribution ($G' > G''$). Water-soluble HEC/CMC polymers can, thus, offer a simple way to improve the flow of MFC suspensions by changing their flocculation behaviour and improving their water retention ability, thereby also modifying and controlling their rheological properties, making them suitable for various applications.

Declarations

References

Agarwal D, MacNaughtan W, Foster TJ (2018) Interactions between microfibrillar cellulose and carboxymethyl cellulose in an aqueous suspension. Carbohydr Polym 185:112–119. https://doi.org/10.1016/j.carbpol.2017.12.086

Agoda-Tandjawa G, Durand S, Gaillard C, Garnier C, Doublier JL (2012) Rheological behaviour and microstructure of microfibrillated cellulose suspensions/low-methoxyl pectin mixed systems. Effect Calcium Ions Carbohydr Polym 87(2):1045–1057. https://doi.org/10.1016/j.carbpol.2011.08.021

Ahmari H, Amiri MC (2015) On the relationship between surface tension and viscosity of fluids. Chem Eng Res Bull 18:18–22. https://doi.org/10.3329/cerb.v18i1.26217

Butchosa N, Zhou Q (2014) Water redispersible cellulose nanofibrils adsorbed with carboxymethyl cellulose. Cellulose 21:4349–4358. https://doi.org/10.1007/s10570-014-0452-7

Cinar Ciftci G, Larsson PA, Riazanova AV, Øvrebø HH, Wågberg L, Berglund LA (2020) Tailoring of rheological properties and structural polydispersity effects in microfibrillated cellulose suspensions. Cellulose 27:9227–9241. https://doi.org/10.1007/s10570-020-03438-6

Clemons C, Sabo R (2021) A review of wet compounding of cellulose nanocomposites. Polymers 13(6):911. https://doi.org/10.3390/polym13060911

Dimic-Misic K, Gane PAC, Paltakari J (2013a) Micro and nanofibrillated cellulose as a rheology modifier additive in CMC-containing pigment-coating formulations. Ind Eng Chem Res 52:16066–16083. https://doi.org/10.1021/ie4028878

Dimic-Misic K, Puisto A, Paltakari J, Alava M, Maloney T (2013b) The influence of shear on the dewatering of high consistency nanofibrillated cellulose furnishes. Cellulose 20:1853–1864. https://doi.org/10.1007/s10570-013-9964-9

Dimic-Misic K, Maloney T, Gane P (2018) Effect of fibril length, aspect ratio and surface charge on ultralow shear-induced structuring in micro and nanofibrillated cellulose aqueous suspensions. Cellulose 25:117–136. https://doi.org/10.1007/s10570-017-1584-3

Facchine EG, Spontak RJ, Rojas OJ, Khan SA (2020) Shear-dependent structures of flocculated micro/nanofibrillated cellulose (MNFC) in aqueous suspensions. Biomacromol 21(9):3561–3570. https://doi.org/10.1021/acs.biomac.0c00586

Haavisto S, Salmela J, Jäsberg A, Saarinen T, Karppinen A, Koponen A (2015) Rheological characterization of microfibrillated cellulose suspension using optical coherence tomography. Tappi J 14:291–302

Hubbe MA, Tayeb P, Joyce M, Tyagi P, Kehoe M, Dimic-Misic K, Pal L (2017) Rheology of nanocellulose-rich aqueous suspensions: a review. BioResources 12:9556–9661

Iotti M, Gregersen ØW, Moe S, Lenes M (2011) Rheological studies of microfibrillar cellulose water dispersions. J Polym Environ 19:137–145

Ishii D, Saito T, Isogai A (2011) Viscoelastic evaluation of average length of cellulose nanofibers prepared by TEMPO-mediated oxidation. Biomacromol 12(3):548–550. https://doi.org/10.1021/bm1013876

Jaiswal AK, Kumar V, Khakalo A, Lahtinen P, Solin K, Pere J, Toivakka M (2021) Rheological behavior of high consistency enzymatically fibrillated cellulose suspensions. Cellulose 28:2087–2104. https://doi.org/10.1007/s10570-021-03688-y

Karim Z, Svedberg A, Lee KY, Hhan MJ (2019) Processing-structure-property correlation understanding of microfibrillated cellulose based dimensional structures for ferric ions removal. Sci Rep 9:10277. https://doi.org/10.1038/s41598-019-46812-6

Karppinen A, Vesterinen AH, Saarinen T, Pietikäinen P, Seppälä J (2011) Effect of cationic polymethacrylates on the rheology and flocculation of microfibrillated cellulose. Cellulose 18:1381–1390. https://doi.org/10.1007/s10570-011-9597-9

Karppinen A, Saarinen T, Salmela J, Laukkanen A, Nuopponen M, Seppälä J (2012) Flocculation of microfibrillated cellulose in shear flow. Cellulose 19:1807–1819. https://doi.org/10.1007/s10570-012-9766-5

Kokol V, Vivod V, Peršin Z, Kamppuri T, Dobnik-Dubrovski P (2021) Screen-printing of microfibrillated cellulose for an improved moisture management, strength and abrasion resistant properties of flame-resistant fabrics. Cellulose 28:6663–6678. https://doi.org/10.1007/s10570-021-03915-6

Koponen AI (2000) The effect of consistency on the shear rheology of aqueous suspensions of cellulose micro- and nanofibrils: a review. Cellulose 27(4):1879–1897. https://doi.org/10.1007/s10570-019-02908-w

Kuijk A, Koppert R, Versluis P, Van Dalen G, Remijn C, Hazekamp J, Nijsse J, Velikov KP (2013) Dispersions of attractive semiflexible fiberlike colloidal particles from bacterial cellulose microfibrils. Langmuir 29:14356–14360

Kumar V, Elfving A, Koivula H et al (2016a) Roll-to-roll processed cellulose nanofiber coatings. Ind Eng Chem Res 55:3603–3613. https://doi.org/10.1021/acs.iecr.6b00417

Kumar V, Nazari B, Bousfield D, Toivakka M (2016b) Rheology of microfibrillated cellulose suspensions in pressure driven flow. Appl Rheol 26:43534. https://doi.org/10.3933/ApplRheol-26-43534

Kumar V, Forsberg S, Engström A et al (2017) Conductive nanographite–nanocellulose coatings on paper. Flex Print Electron 2:35002. https://doi.org/10.1088/2058-8585/aa728e

Lauri J, Haavisto S, Salmela J, Miettinen A, Fabritius T, Koponen AI (2021) Online measurement of floc size, viscosity, and consistency of cellulose microfibril suspensions with optical coherence tomography. Cellulose 28:3373–3387

Lee BB, Chan ES, Ravindra P, Khan TA (2012) Surface tension of viscous biopolymer solutions measured using the Du Nouy ring method and the drop weight methods. Polym Bull 69:471–489. https://doi.org/10.1007/S00289-012-0782-2

Li MC, Wu Q, Moon RJ, Hubbe MA, Bortner MJ (2021) Rheological aspects of cellulose nanomaterials: governing factors and emerging applications. Adv Mater 33(21):2006052. https://doi.org/10.1002/adma.202006052

Lundahl MJ, Klar V, Wang L, Ago M, Rojas OJ (2017) Spinning of cellulose nanofibrils into filaments: a review. Ind Eng Chem Res 56:8–19. https://doi.org/10.1021/acs.iecr.6b04010

Mariani LM, Johnson WR, Considine JM et al (2019) Printing and mechanical characterization of cellulose nanofibril materials. Cellulose 26:2639–2651. https://doi.org/10.1007/s10570-019-02247-w

Medronho B, Romano A, Miguel MG, Stigsson L, Lindman B (2012) Rationalizing cellulose (in)solubility: reviewing basic physicochemical aspects and role of hydrophobic interactions. Cellulose 19:581–587. https://doi.org/10.1007/s10570-011-9644-6

Miller AF, Donald AM (2002) Surface and interfacial tension of cellulose suspensions. Langmuir 18(26):10155–10162

Moberg T, Sahlin K, Yao K, Geng S, Westman G, Zhou Q, Oksman K, Rigdahl M (2017) Rheological properties of nanocellulose suspensions: effects of fibril/particle dimensions

and surface characteristics. Cellulose 24:2499–2510. https://doi.org/10.1007/s10570-017-1283-0

Naderi A, Lindström T (2014) Carboxymethylated nanofibrillated cellulose: effect of monovalent electrolytes on the rheological properties. Cellulose 21:3507–3514. https://doi.org/10.1007/s10570-014-0394-0

Naderi A, Lindström T (2015) Rheological measurements on nanofibrillated cellulose systems: a science in progress. In: Mondal MIH (ed) Cellulose and cellulose derivatives. Nova Science Publishers Inc, Hauppauge, pp 187–202

Nazari N, Kumar V, Bousfield DW, Toivakka M (2016) Rheology of cellulose nanofibers suspensions: boundary driven flow. J Rheol 60:1151–1159. https://doi.org/10.1122/1.4960336

Nechyporchuk O, Belgacem MN, Pignon F (2014) Rheological properties of micro/nanofibrillated cellulose suspensions: wall-slip and shear banding phenomena. Carbohydr Polym 112:432–439. https://doi.org/10.1016/j.carbpol.2014.05.092

Nechyporchuk O, Belgacem MN, Pignon F (2016) Current progress in rheology of cellulose nanofibril suspensions. Biomacromol 17:2311–2320. https://doi.org/10.1021/acs.biomac.6b00668

Oh K, Lee JH, ImW, et al (2017) Role of cellulose nanofibrils in structure formation of pigment coating layers. Ind Eng Chem Res 56:9569–9577. https://doi.org/10.1021/acs.iecr.7b02750

Pääkkö M, Ankerfors M, Kosonen H, Nykänen A, Ahola S, Österberg M, Ruokolainen J, Laine J, Larsson PT, Ikkala O, Lindström T (2007) Enzymatic hydrolysis combined with mechanical shearing and high-pressure homogenization for nanoscale cellulose fibrils and strong gels. Biomacromol 8(6):1934–1941

Pääkkönen T, Dimic-Misic K, Orelma H et al (2016) Effect of xylan in hardwood pulp on the reaction rate of TEMPO-mediated oxidation and the rheology of the final nanofibrillated cellulose gel. Cellulose 23:277–293. https://doi.org/10.1007/s10570-015-0824-7

Saarikoski E, Saarinen T, Salmela J, Seppälä J (2012) Flocculated flow of microfibrillated cellulose water suspensions: an imaging approach for characterisation of rheological behavior. Cellulose 19:647–659. https://doi.org/10.1007/s10570-012-9661-0

Schenker M, Schoelkopf J, Gane P et al (2018) Influence of shear rheometer measurement systems on the rheological properties of microfibrillated cellulose (MFC) suspensions. Cellulose 25:961–976. https://doi.org/10.1007/s10570-017-1642-x

Schenker M, Schoelkopf J, Gane P, Mangin P (2019) Rheology of microfibrillated cellulose (MFC) suspensions: influence of the degree of fibrillation and residual fibre content on flow and viscoelastic properties. Cellulose 26:845–860. https://doi.org/10.1007/s10570-018-2117-4

Shafiei-Sabet S, Martinez M, Olson J (2016) Shear rheology of micro-fibrillar cellulose aqueous suspensions. Cellulose 23:2943–2953. https://doi.org/10.1007/s10570-016-1040-9

Sviderskyi V, Melnyk L, Shendera A, Fleisher H (2018) Rheological properties of polymer colloid–cellulose thickener systems. Chem Chem Technol 12(2):207–212

Taheri H, Samyn P (2016) Effect of homogenization (microfluidization) process parameters in mechanical production of micro- and nanofibrillated cellulose on its rheological and morphological properties. Cellulose 23:1221–1238. https://doi.org/10.1007/s10570-016-0866-5

Vadodaria SS, Onyianta AJ, Sun D (2018) High-shear rate rheometry of micro-nanofibrillated cellulose (CMF/CNF) suspensions using rotational rheometer. Cellulose 25:5535–5552. https://doi.org/10.1007/s10570-018-1963-4olV)

Veen SJ, Versluis P, Kuijk A, Velikov KP (2015) Microstructure and rheology of microfibril-polymer networks. Soft Matter 11:8907–8912. https://doi.org/10.1039/C5SM02086G

Vesterinen AH, Myllytie P, Laine J, Seppälä J (2010) The effect of water-soluble polymers on rheology of microfibrillar cellulose suspension and dynamic mechanical properties of paper sheet. J Appl Polym Sci 116:2990–2997

Wang X, Wang Q, Xu C (2020) Nanocellulose-based inks for 3d bioprinting: key aspects in research development and challenging perspectives in applications - a mini review. Bioengineering 7(2):40. https://doi.org/10.3390/bioengineering7020040

Yuan T, Zeng J, Wang B, Cheng Z, Chen K (2021) Cellulosic fiber: mechanical fibrillation-morphology-rheology relationships. Cellulose 28:7651–7662. https://doi.org/10.1007/s10570-021-04034-y